

Mechanism Study on Formation of Initial Condensate Droplets

Liu Tianqing, Mu Chunfeng, Sun Xiangyu, and Xia Songbai

Dept. of Chemical Engineering, Dalian University of Technology, Dalian 116012, China

DOI 10.1002/aic.11124

Published online February 16, 2007 in Wiley InterScience (www.interscience.wiley.com).

Keywords: initial condensation, nucleation, mechanism, EPMA, magnesium

Introduction

Condensation is an important and widely accepted heat transfer type in lots of industries and engineering processes, such as petrochemical industry, power industry, air conditioning, and refrigerating process. And the heat transfer coefficient of dropwise condensation is much higher than that of filmwise condensation. It is therefore undisputed that the size of the heat exchangers and/or the energy consumption rate can be greatly reduced if dropwise condensation can be realized in those industries and processes.

Dropwise condensation was first discovered by Schmidt et al.¹ in 1930s. Since then, many scientists and researchers, such as Tanasawa,² Rose,^{3–5} Westwater,⁶ and Umur and Griffith,⁷ have made lots of contributions in the theory and experimental investigation of dropwise condensation. Even though, lots of problems and difficulties for dropwise condensation still exist.

To realize a long stable dropwise condensation, the heat transfer surfaces must be effectively treated and modified, which can be achieved only after we clearly understand the mechanism for the formation of initial condensate drops of dropwise condensation process. Two kinds of hypotheses for the mechanism still exist: liquid film fracture hypothesis and surface nucleation site hypothesis. The former one was first proposed by Jakob⁸ in 1936. It describes that a thin condensate film will form on a cool surface when vapor contacts the surface, and the film increases in its thickness as the vapor condenses until broken when its thickness reaches a critical value. The fractured film will form the initial liquid drops with the action of surface tension. Ruckenstein and

Metiu⁹ and Haraguchi¹⁰ tried to support this hypothesis with their work. Ruckenstein and Metiu⁹ considered that the condensation surface contained numerous active centers so close as to form a continuous film of the condensate. And they found the critical thickness of the fractured film to be about 0.27 μm and the critical time to form the critical film to be in the magnitude of 10^{-2} s through the thermodynamic calculations. Haraguchi¹⁰ applied microscopy technology and observed the initially formed droplet size to be about 1 μm and the critical thickness of the fractured condensate film to be 0.1–0.3 μm .

The second hypothesis, surface nucleation site mechanism, was proposed by Tammann and Boehme.¹¹ It considered that dropwise condensation was a nucleation process with nuclei randomly existing on solid surfaces. McCormick and Westwater,^{12,13} Peterson and Westwater,¹⁴ and Umur and Griffith⁷ all proved the evidence of droplet nucleation and identified the nucleation sites during dropwise condensation with microscope and movie cameras.

Although there have been lots of researches for the mechanism of the formation of initial drops of dropwise condensation, the experimental methods used only included microscopy and high speed camera.^{7,10,12–18} And these methods were limited to investigate the microscale phenomena (size greater than 0.1 μm) no matter for the detection of initial condensate drops or films on condensation surfaces. According to the calculation of thermodynamics on new phase formation, however, the size of an initial liquid nucleus is in nanometer scale if the initial condensate forms in nucleation state. Therefore, we should try to detect the initial liquid nucleus in nanoscale if we consider the surface nucleation hypothesis to be correct. Otherwise we should try to identify the initial liquid film with the thickness in nanoscale and prove that this film increases in its thickness till the critical value (0.1–0.3 μm)¹⁰ and then fractures if we want to prove

Correspondence concerning this article should be addressed to Liu Tianqing at liutq@dlut.edu.cn.

the hypothesis of liquid film fracture is true. Unfortunately, nothing is known so far for the initial condensation process from nanometer to micrometer size.

It is thus clear that the initial condensate state in nanometer magnitude must be identified no matter which hypothesis is correct; namely, the test result of the initial condensation state in the scale less than 0.1 μm becomes the key for the mechanism of initial liquid drop formation of dropwise condensation. Since it is almost impossible to directly observe the initial condensation in nanometer scale in situ with current instruments, there is no experimental result for the initial steam condensation in this scale to date. Novel experimental route should be designed to realize the detection of the initial condensation state in nanoscale.

In this study magnesium surfaces that can react with hot water were prepared first. Then, the initial condensation of steam on the magnesium surfaces was achieved by controlling the subcooling and the contacting time between the steam and the magnesium surface. Since the condensate was hot, it can react with magnesium to produce magnesium hydroxide. Hence the chemical composition of the condensation surface changed. The variation of the chemical composition on the surface depends on the initial condensate state so that the marker of the initial condensation state could remain on the surfaces. Afterwards electron probe microanalyzer (EPMA) was applied to analyze the variation of the chemical composition of the surfaces before and after condensation, which can be used to deduce the initial condensation state.

Experimental Design and Methods

Experimental fundamentals

Magnesium can react with hot water, i.e. $\text{Mg} + 2\text{H}_2\text{O}$ (hot water) $= \text{Mg}(\text{OH})_2 + \text{H}_2\uparrow$, while the reaction will be very slow if the reactant is steam and the later reaction can be neglect during short time. If we use metal magnesium as the condensation surface, the hot condensate of steam will react with magnesium. Thus the chemical composition of the local surface where the condensate forms will change. Besides, the initial liquid droplet formation of dropwise condensation on the magnesium surfaces can be achieved by controlling the subcooling and the contacting time between the steam and the magnesium surface. In this case, the chemical reaction and thus the variation of the chemical composition will take place only at places where the initial condensate nuclei and liquid drops form, while the chemical composition on the other places without liquid formation will not change, if the surface nucleation hypothesis is correct. That is, the distribution of oxygen element on the surface should not be uniform. On the other hand, if the hypothesis of liquid film fracture is true, the condensation surface will be covered by a thin condensate film during the initial condensation, and the chemical reaction on the surface will take place uniformly, i.e., the distribution of oxygen element on the surface should be uniform. Therefore, we can deduce the mechanism of initial drop formation afterwards through identifying the oxygen distribution state on the surface.

Experimental apparatus

The apparatus used for the initial condensation in the experiments is shown in Figure 1. It consists of condensation

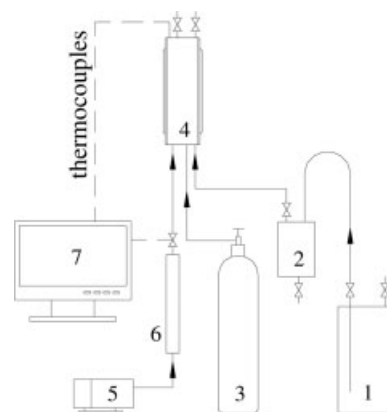


Figure 1. Experiment: 1, steam generator; 2, vapor-liquid segregator; 3, nitrogen gas; 4, condensation chamber; 5, air pump; 6, air heater; 7, computer.

chamber, air heating, steam generation, nitrogen protection and data collection and control.

1. *Condensation chamber:* Its structural diagram is shown in Figure 2. It mainly consists of the baseboard and front and back covers. The baseboard and the covers are made from poly(tetrafluoroethylene) and polycarbonate respectively. The outer size of the chamber is 15 cm in diameter and 5 cm in thickness. Four holes were opened on the baseboard with 1 cm in diameter. The test coupons made of magnesium with 3 mm in thickness were inlaid in these holes. On the back of each coupon a 0.3-mm small hole was drilled to insert a thermocouple for temperature measurement. There are inlets and outlets on the back side and front side for air and steam or nitrogen gas respectively. The air flowed in the back side while steam or nitrogen flowed in the front side. The condensation of steam on the test surfaces could be viewed through the front cover.
2. *Air heating:* The air at room temperature was pumped by an air compressor and flowed through a rotameter and the electric heater. The temperature of exit air can be controlled with the input power of the heater. The hot air entered the back channel of the condensation chamber, contacted the back surfaces of the magnesium coupons which had been fixed in the condensation chamber, and made the temperature of the coupons rise to the set value. The set temperature of the coupons was lower than the temperature of steam, thus we could obtain the needed subcooling. The hot air entered the atmosphere when it left the back place of the chamber.
3. *Steam generation:* A 1-l flask filled with 80% water was put in an electric heating jacket. Steam can be generated by inputting proper power to the jacket. The steam entered the vapor-liquid separator before it flowed into the condensation chamber, where part of the steam condensed on the coupon surfaces and the remaining steam exited the chamber into the atmosphere.
4. *Nitrogen protection:* Nitrogen from a nitrogen bottle flowed through the condensation chamber with low flow rate so that the magnesium coupons fixed in the chamber

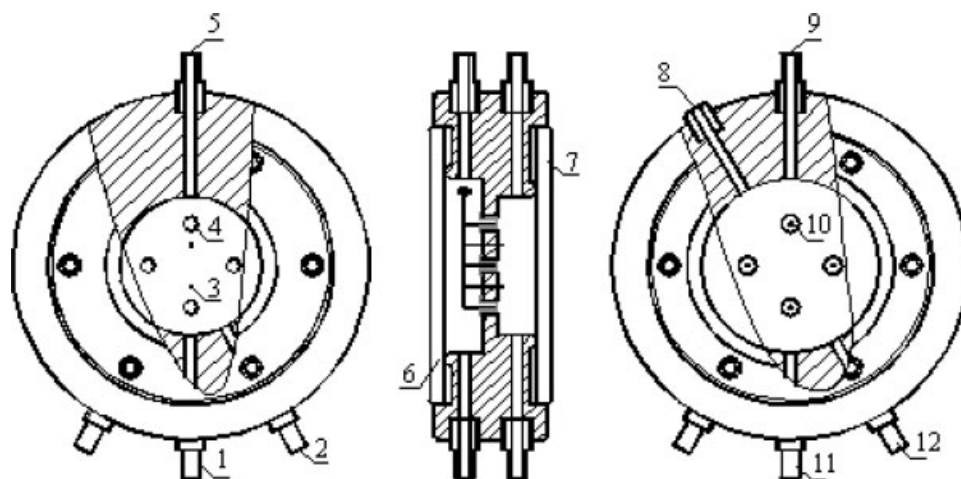


Figure 2. Structural diagram of condensation chamber: 1, condensate drainage; 2, steam inlet; 3, thermocouples in the chamber; 4, coupons; 5, vent of steam or nitrogen; 6, back cover; 7, front cover; 8, hole for thermocouple wires; 9, air outlet; 10, thermocouples in coupons; 11, air inlet; 12, nitrogen inlet.

could be protected against oxidization before and after they contacted with steam.

5. *Data collection and control:* The thermocouples and the relative electromagnetic valves were linked to a computer with a data collecting and controlling board. And a visual basic program was used to collect temperature and control the valves.

Test methods of initial condensation and related parameters

Nitrogen began to flow through the condensation chamber after the magnesium coupons were fixed in the chamber. Then, the air pump and the heater were switched on to make the heated air flow through the back channel of the condensation chamber. When the temperature of the coupons reached the set value and the system became stable, nitrogen was shut off and steam began to flow into the chamber for the designed period. After that, steam was stopped and replaced with nitrogen again. In this way, the initial condensation on the coupon surfaces with different subcoolings and different condensation time could be realized. The related parameters of the tests are summarized in Table 1.

Preparation of magnesium surfaces

Magnetic-control sputtering (MCS), a novel plating film technology with high speed and low temperature, was used to prepare the magnesium surfaces. The multifunction and ultrahigh vacuum system (Shenyang instrument plant, China) was applied to deposit the magnesium film on the monocrystalline silicon substrate. The substrate and the magnesium target with purity of 99.999% were completely cleaned before plating the film. The diameter of the magnesium target was 60 mm. The working pressure in the plating chamber was 0.5 Pa, the substrate was in room temperature, and the sputtering power was 100 W. The plating time was 1.5 h.

Characterization of the magnesium surface topography

The topography of the magnesium surfaces prepared and their surface roughness were characterized with the atomic

force microscope (AFM, PicoPlus, Molecular Imaging Company, US). The average value of three location measurements randomly selected on each surface was taken as the average roughness for the surface. The thickness of the magnesium film plated with MCS method was measured with the EPMA (EPMA-1600, shimadzu, Japan).

Measurement of chemical composition of the material surface

The chemical compositions of magnesium and oxygen on the test surfaces as well as their variations before and after condensation were measured with the EPMA (EPMA-1600) by randomly selecting the micro areas on the surfaces. Also, the distributions of these elements on the surfaces were scanned with the instrument. The measurement principle of an EPMA is that the characteristic X-ray of an element on the sample surface can be excited out with the incidence of a finely focused electron beam. Then the kinds and contents of elements on the sample surface can be identified by analyzing the wavelength and intensity of the X-ray respectively. In this way we can determine where the condensate reacted with the magnesium and whether the reaction was uniform.

Table 1. Experimental Parameters and Oxygen Contents on Magnesium Surfaces Before and After Initial Condensation

Coupon No.	Average Subcooling, °C	Condensation Time, s	Oxygen Content, wt %
1	—	—	0
2	2.7	10	5.27
3	4.6	10	9.04
4	4.9	10	11.17
5	4.6	20	11.56
6	6.1	60	16.11
7	9.3	30	20.57
8	2.1	5	2.21
9	0.8	10	3.45
10	1.9	10	3.56
11	15.2	60	50.1

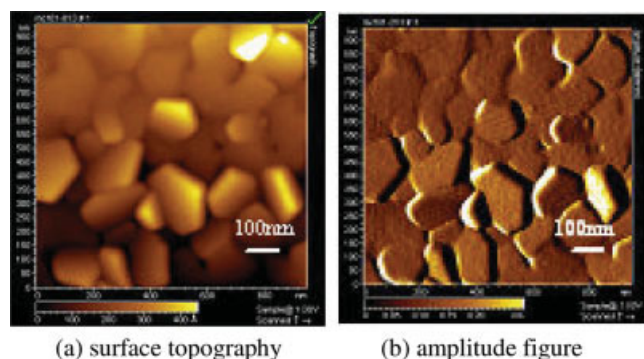


Figure 3. AFM photomicrographs of no. 1 surface in Table 1, average roughness 23 nm.

(a) Surface topography; (b) amplitude figure. [Color figure can be viewed in the online issue, which is available at www.interscience.wiley.com.]

The minimum scanned analyzed area could be $1\ \mu\text{m} \times 1\ \mu\text{m}$.

Results and Discussion

Surface topography and roughness of magnesium coupons

The AFM-scanned surface topography and roughness of the magnesium coupons prepared with MCS are shown in Figure 3. It can be seen that the magnesium film on the substrate of the monocrystalline silicon consists of magnesium particles sized from 50 to 100 nm. The film is dense and the distribution of the fine particles is uniform. The average roughness of the surface is about 23 nm. Moreover, the section of the substrate and the film was scanned with EPMA,

and the result showed that the thickness of the plated film was $21\ \mu\text{m}$, which meant that the substrate surface was completely covered by magnesium. Therefore, the magnesium surfaces prepared with the MCS could be used in the followed condensation experiments.

Distribution of oxygen on magnesium surface before and after condensation

The distributions of oxygen and magnesium on the test surfaces were measured with EPMA before and after the initial condensation under different subcooling and different condensation time. The EPMA-scanned results under micrometer scale are shown in Figure 4. We can find that very little oxygen distributes uniformly on the magnesium surface (Coupon 1 in Table 1) before the condensation test. After the condensation, however, it appears nonuniform on the surfaces and the content increases apparently with subcooling and condensation time (oxygen content increases from Coupons 2–7 in Table 1).

In order to investigate the distribution of oxygen on the magnesium surfaces after more initial condensation under nanometer scale, the condensation tests were carried out with lower subcooling and shorter condensation time (Coupons 8–10 in Table 1). After that, $1\ \mu\text{m} \times 1\ \mu\text{m}$ areas were scanned on these surfaces with EPMA. The local area in the pictures obtained in this scale were further enlarged 10 times with the Photoshop software, and the size and the distribution of the initial condensate nuclei were gained in this way, which are shown in Figure 5. It is thus clear that the size of the initial condensate nuclei was in the range of 3–10 nm, which agrees well with the calculated result of the thermodynamics for new phase formation.

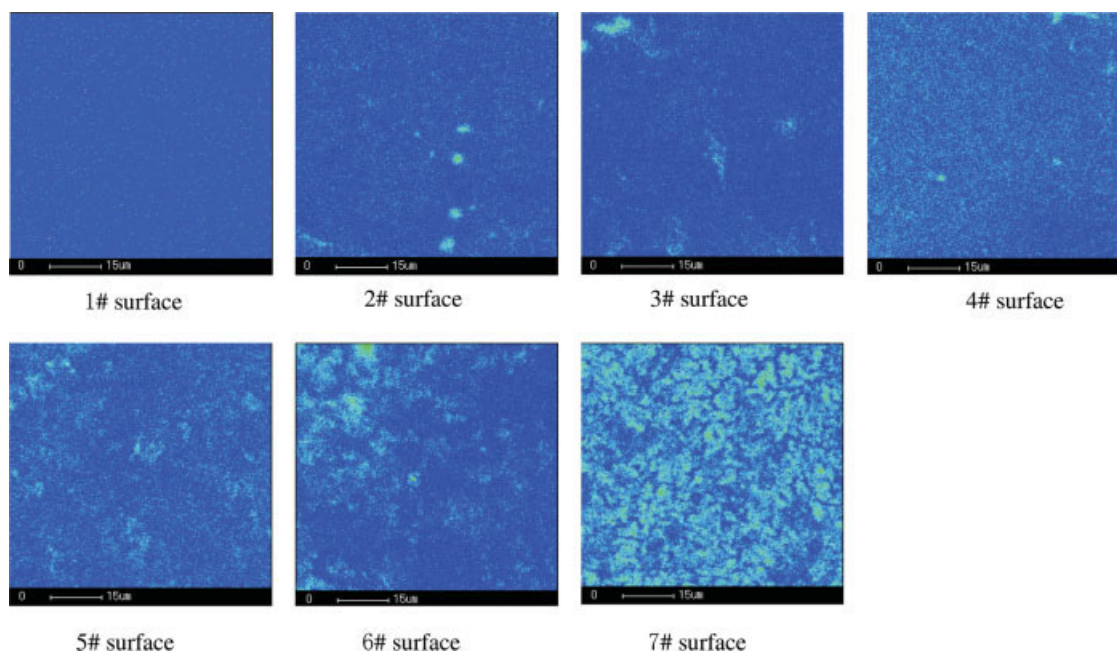


Figure 4. Distributions of oxygen and magnesium on MCS surfaces in microscale, EPMA-scanned area – $60\ \mu\text{m} \times 60\ \mu\text{m}$. Green color: oxygen; blue color: magnesium.

[Color figure can be viewed in the online issue, which is available at www.interscience.wiley.com.]

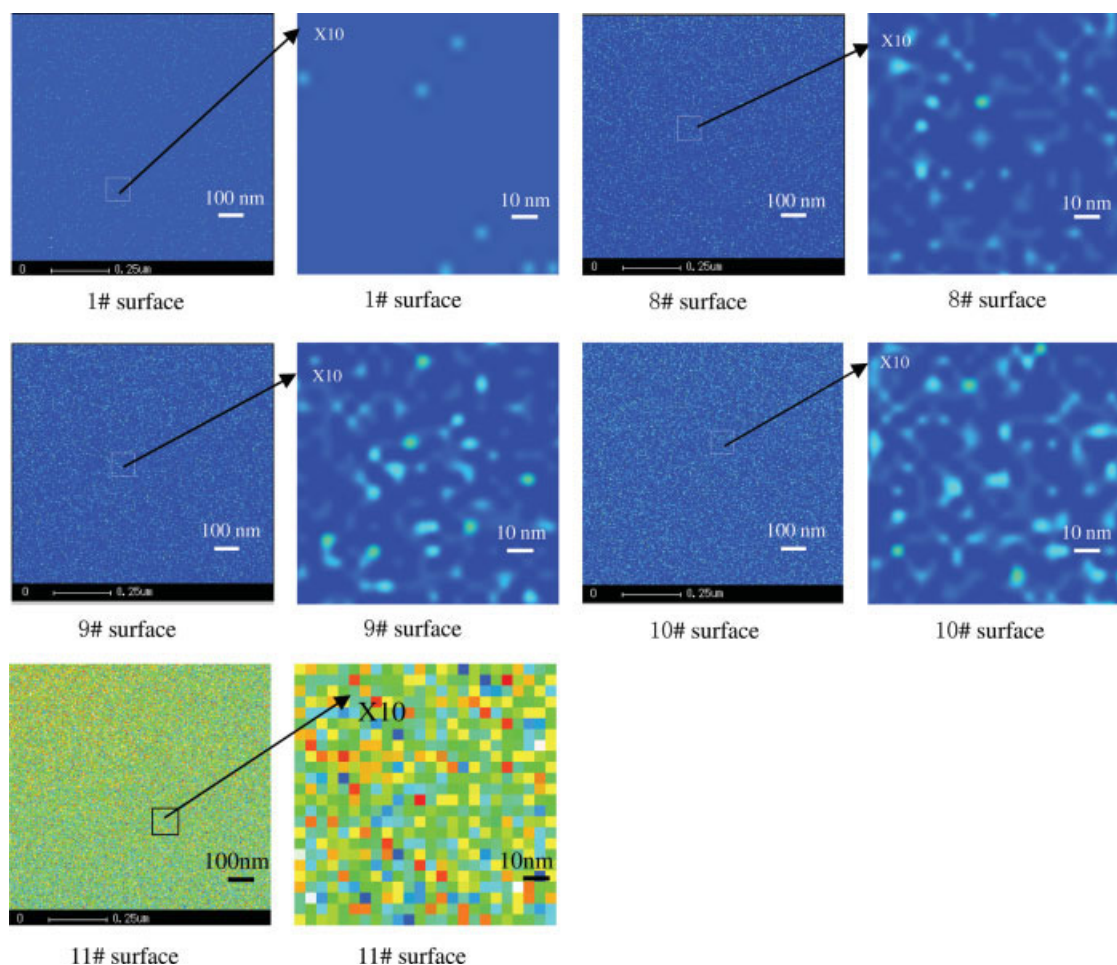


Figure 5. Distributions of oxygen and magnesium on MCS surfaces in nanoscale, EPMA-scanned area – $1\ \mu\text{m} \times 1\ \mu\text{m}$. Blue color: magnesium, green and other color: oxygen.

[Color figure can be viewed in the online issue, which is available at www.interscience.wiley.com.]

It should be pointed out that the initial condensate nuclei must be separated by sufficient distance so that they may be distinguished with EPMA. According to the results of the model and experiment of Rose,¹⁹ the number of nucleation sites for dropwise condensation is $10^9 - 10^{11}/\text{cm}^2$. On the basis of this figure, the average distance between nucleation sites is greater than 30 nm, i.e., the distance between the edges of two condensate nuclei is larger than 10 nm, which is sufficient for an EPMA to identify. Meanwhile it can be seen from Figure 5 that there is clear blue area on the surface (Coupons 8–10), that is, the average distance between initial condensate drops indeed is greater than 10 nm. On the other hand, these clear gaps between nuclei would disappear if there was a liquid film on the surface.

To compare the oxygen distribution on the above-mentioned dropwise condensation surfaces with that on a surface after filmwise condensation, Coupon 11 in Table 1 was used to undertake a filmwise condensation by means of a larger subcooling and its surface oxygen distribution is shown in Figure 5. We can see that the oxygen distribution on this surface is quite different from that on the others. And there is oxygen almost everywhere on this surface since it was covered by the condensate film and the

chemical reactions took place on the whole surface. There is no blue area (condensate-uncovered area) anymore. The different colors, such as green, yellow, and red, on this surface only mean different oxygen contents at certain positions.

It should also be pointed out that a thin uniform condensate film would still cause the surface to be oxidized uniformly even if the roughness scale of the surface is 20–30 nm in case the liquid film fracture hypothesis happened. This is because the critically fractured film thickness is $0.1 - 0.3\ \mu\text{m}$ ¹⁰, which is thick enough to submerge the surface with 20–30 nm in roughness. Therefore, if the initial condensation took place in liquid film fracture, the oxygen distribution of the surface would be similar to that of Coupon 11 in Figure 5. However, what really happened is not like this. As a result the initial condensate drops formed on the cool surface did not result from the fractured thin liquid film.

Conclusions

The relatively smooth magnesium surfaces were prepared with the method of MCS. The average roughness of the surfaces is 20 nm.

The initial condensation for the dropwise condensation process was performed on the magnesium surfaces under different subcoolings and condensation time. The results of surface composition analyzed with EPMA in different scales indicate that the initial condensate only forms on the certain positions of solid surfaces when steam condensates on the magnesium surfaces. And the distribution of the sites forming condensate drops is not uniform. The size of the initial condensate nuclei is in the range of 3–10 nm, which agrees well with the calculation of thermodynamics for new phase formation. The state of initial condensate formed on the surfaces is not in thin film but in nuclei. All these results demonstrate that the mechanism of formation of initial condensate drops for dropwise condensation accords with the hypothesis of nucleation sites.

Acknowledgment

This work was supported by the National Natural Science Foundation of China (50376006).

Literature Cited

- Schmidt E, Schurig W, Sellschop W. Versuche über die kondensation von wasserdampf in film- und tropfenform. *Tech Mech Thermodyn*. 1930;1:53–63.
- Tanasawa I. Recent advances in condensation heat transfer. *Proc 10th Int Heat Transfer Conf*. 1994;1:197–312.
- Rose JW. Dropwise condensation theory and experiment: a review. *Proc IME J Power Energ*. 2002;216:115–128.
- Rose JW. Interphase matter transfer, the condensation coefficient and dropwise condensation. *Proc 11th Int Heat Transfer Conf*. 1998;1:89–104.
- Rose JW. Dropwise condensation theory. *Int J Heat Mass Transfer*. 1981;24:191–194.
- Westwater JW. Condensation. In: *US-Japan Cooperative Science Program. Condensation Heat Transfer in Energy Problems*. Mizuchina T, Yang WJ, eds. Washington, DC: Hemisphere, 1983:81–92.
- Umur A, Griffith P. Mechanism of dropwise condensation. *J Heat Transfer*. 1965;87:275–282.
- Jakob M. Heat transfer in evaporation and condensation. *Mech Eng*. 1936;58:729–739.
- Ruckenstein E, Metiu H. On dropwise condensation on the solid surface. *Chem Eng Sci*. 1965;20:173–179.
- Haraguchi T. Microscope observations of the initial droplet formation mechanism in dropwise condensation. *Heat Transfer Japan Res*. 1992;21:573–585.
- Tammann G, Boehme W. Die Zahl der wassertropfchen bei der kondensation auf verschiedenen festen stoffen. *Ann Physik*. 1935;5:77–80.
- McCormick JL, Westwater JW. Nucleation sites for dropwise condensation. *Chem Eng Sci*. 1965;20:1021–1031.
- McCormick JL, Westwater JW. Drop dynamics and heat transfer during dropwise condensation of water vapor. *Chem Eng Prog Symp Ser*. 1966;62(64):120–134.
- Peterson AC, and Westwater JW. Dropwise condensation of ethylene glycol. *Chem Eng Prog Symp Ser*. 1966;62(64):135–142.
- Graham C, Griffith P. Drop size distributions and heat transfer in dropwise condensation. *Int J Heat Mass Transfer*. 1973;16:337–346.
- Song Y, Xu D, Lin J. Study on dropwise condensation mechanism. *J Chem Eng Chin Univ*. 1990;4:240–246.
- Tanaka H. Measurements of drop-size distributions during transient dropwise condensation. *J Heat Transfer Trans ASME*. 1975;97:341–346.
- Peter C, Wayner Jr. Nucleation, growth and surface movement of a condensing sessile droplet. *Colloids Surf A*. 2002;206:157–165.
- Rose JW. Further aspects of dropwise condensation theory. *Int J Heat Mass Tran*. 1976;19:1363–1370.

Manuscript received May 16, 2006, revision received Nov. 9, 2006, and final revision received Jan. 3, 2007.